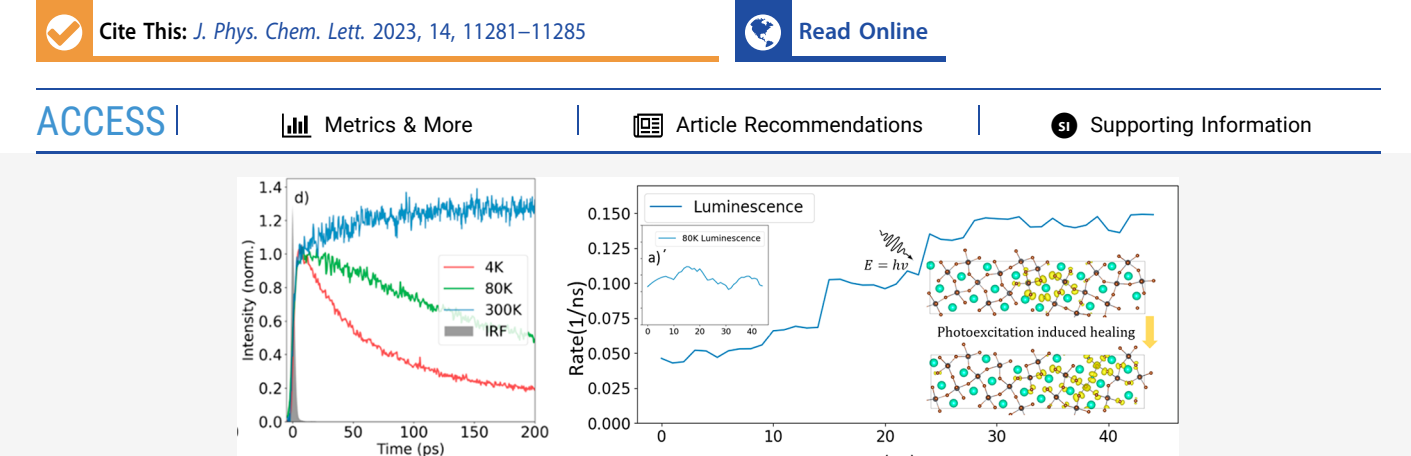


pubs.acs.org/JPCL Letter

Breaking the Condon Approximation for Light Emission from Metal Halide Perovskite Nanocrystals

Dallas Strandell, Yifan Wu, Carlos Mora-Perez, Oleg Prezhdo, and Patanjali Kambhampati*



ABSTRACT: The idea that the electronic transition dipole moment does not depend upon nuclear excursions is the Condon approximation and is central to most spectroscopy, especially in the solid state. We show a strong breakdown of the Condon approximation in the time-resolved photoluminescence from CsPbBr₃ metal halide perovskite semiconductor nanocrystals. Experiments reveal that the electronic transition dipole moment increases on the 30 ps time scale due to structural dynamics in the lattice. *Ab initio* molecular dynamics calculations quantitatively reproduce experiments by considering excitation-induced structural dynamics.

Time(ps)

The idea that the electronic transition moment is independent of nuclear excursions is central to most of spectroscopy, especially in condensed matter systems, and is termed the Condon approximation. While there are glimpses of the breakdown of the Condon approximation in the dynamics of small molecules, this approximation is especially central to analysis of spectroscopy of the condensed matter^{2–4} due to weaker coupling to phonons, i.e., electronic structural dynamics. Yet the extent to which the transition moment depends upon nuclear motion is central to how one analyzes their spectroscopy and dynamics. This breakdown reflects strong electron—nuclear interactions from which structural dynamics can be understood.

In small molecular systems there have been experiments that focus on the breakdown of the Condon approximation via indirect spectroscopic means such as Raman spectroscopy^{5–7} or other frequency domain methods^{8,9} under the guise of nonadiabatic dynamics which arises from the breakdown of the Born–Oppenheimer approximation^{10,11} which is related to the Condon approximation by the nuclear coordinate derivatives. With the advent of femtosecond lasers, it was possible to directly observe non-Condon effects in the time domain via amplitude modulations of time-resolved photoluminescence (t-PL) spectra or transient absorption (TA) spectra. ^{12–14} Even in small molecules, these observations of amplitude modulation due to non-Condon dynamics are rare compared to frequency modulation by Franck–Condon-based wavepacket dynam-

ics.^{15–17} In condensed matter systems such as graphene and carbon nanotubes, there has surprisingly been identification of the breakdown of the Condon approximation via indirect observation by interpretation of Raman spectra,^{3,4} like in molecular systems. What is missing is a direct, time-domain measurement of the breaking down of the Condon approximation in a condensed matter system.

Semiconductor metal halide perovskites, and especially their nanocrystal (MHP NC) form, provide a platform to investigate electronic structural dynamics such as non-Condon effects due to their rich structural dynamics and strong electron—lattice interactions and novel properties that have given rise to their remarkable performance in devices. ^{18–23} Due to their unique lattice that is ionic rather than covalent, perovskites can exhibit liquid—solid duality in terms of their being a phonon glass/electron crystal. ^{24–27} Being a phonon glass, their structural dynamics takes place on a distribution of time scales from 300 fs for polaron formation ²⁸ to 30 ps for other lattice dynamics ^{25,29–33} in the cascade of processes that parallels solvation dynamics in liquids and glasses. ^{34,35}

Received: October 10, 2023 Revised: November 22, 2023 Accepted: December 6, 2023 Published: December 7, 2023





Here, we show a strong breakdown of the Condon approximation in the t-PL spectroscopy of a model perovskite system of 15 nm CsPbBr3 nanocrystals, the model system that has been most studied to date. The Condon approximation of the independence of the electronic transition dipole moment to lattice structural dynamics is one of the central approximations in condensed matter physics. This breaking of the Condon approximation is revealed by the timedependent excited-state survival probabilities being highly nonexponential at sufficiently low excitation densities as reflected in the t-PL signals. Rather than reveal a prompt decay as anticipated from most systems, the t-PL shows a surprising buildup time of 30 ps in which the t-PL increases in amplitude by 20%. This buildup of the t-PL area is not due to hot-carrier emission. It is proposed to arise from the glassy structural dynamics unique to perovskites. Comparison to covalent CdSe nanocrystals and a molecular laser dye show no such delayed-buildup effects, consistent with their following the Condon approximation. Theory performed at the ab initio molecular dynamics level quantitatively reproduces experiment and rationalizes these results in terms of excitation-induced structural dynamics.

Figure 1 presents an overview of the system and the spectroscopy. Figure 1a shows the CsPbBr₃ metal halide perovskite forms with APbX3 stoichiometry, in which the lattice consists of covalent PbX₃⁻ cubic-to-nearly cubic framework filled with an A+ cation, where A+ corresponds to Cs⁺, formamidinium, or methylammonium and X corresponds to a halide anion. The main point from the structural analysis is that these structures are both very polar with strong electron lattice couplings, and there is a broad distribution of glassy and low-frequency phonon modes that characterize the system. At 300 K, one generally sees spectral densities rather than wellresolved peaks, consistent with their glassy lattice.³⁴ Figure 1b shows a linear absorption and PL spectrum of the 15 nm MHP NC. These NC are twice the 7 nm Bohr length and can be considered weakly confined or bulk-like NC, 22,23 rather than strongly confined quantum dots (QD) as in the case of CdSe, which is smaller than its Bohr length.

Figure 1c,d shows the t-PL data obtained using a streak camera detector with a time resolution (instrument response function, IRF) of 3 ps when in the ps mode. The IRF is 100 ps in the ns mode. The step size in the ps mode is 330 fs. Spectrally resolved and spectrally integrated measurements were obtained at a range of pump fluences and temperatures, using a liquid He cryostat (see the Supporting Information for details). The t-PL on the nanosecond time scale shows no spectral dynamics, and the population decay is observed to be single exponential on the nanosecond time scale, consistent with the literature.

The question of monitoring the breakdown of the Condon approximation in real time is illustrated in Figure 1e-h. In molecular systems, there are several indirect ways to observe non-Condon effects, such as details of the Raman scattering process. But these are indirect evidence of non-Condon effects in contrast to real-time observations that are made possible in time domain measurements, whether transient absorption (TA) or t-PL. In the case of a molecular system with a high-frequency quantum mode one will observe coherent wave-packet dynamics that is oscillatory and underdamped due to the nature of the dynamics (Figure 1e). In the case of a low-frequency classical mode, one will see diffusive motion along the excited-state potential energy surface in the vein of

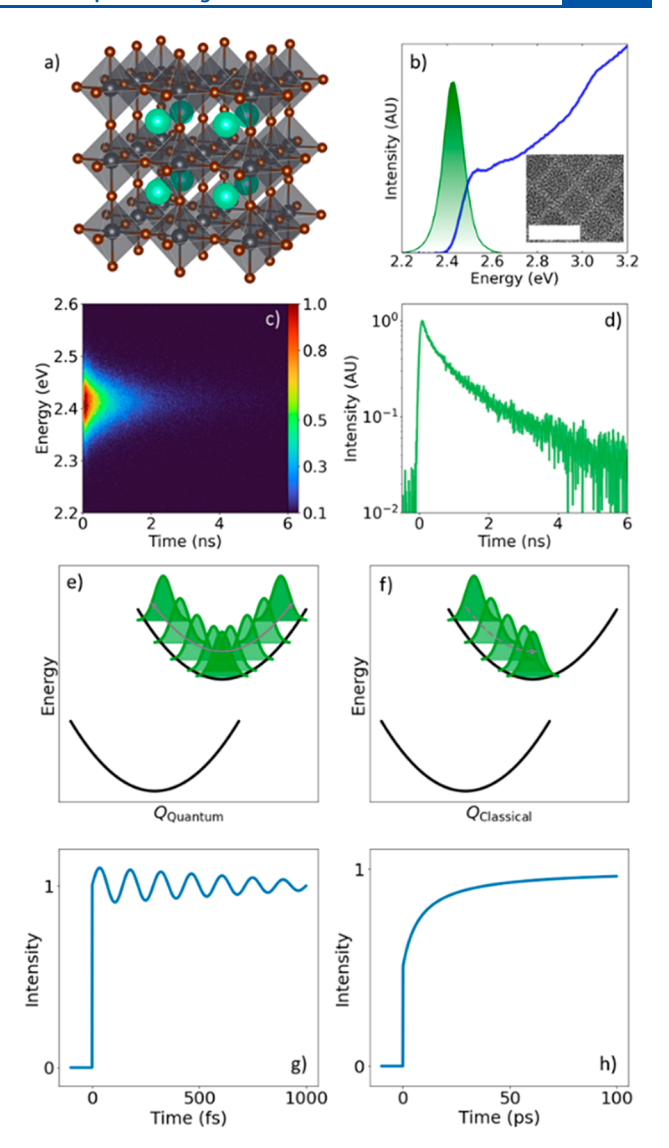


Figure 1. Observing the breakdown of the Condon approximation in limiting cases. (a) The $CsPbBr_3$ perovskite nanocrystals have an ionic, glassy crystal structure as schematically illustrated and have an edge length of 15 nm. (b) The steady-state absorption spectra are featureless, with a Stokes shifted photoluminescence (PL) band. The inset shows a transmission electron microscopy image with a 20 nm scale bar. The time-resolved PL (t-PL) spectrum is shown in (c), and the spectrally integrated kinetic transient is shown in (d). The breakdown of the Condon approximation can be observed in the limits of coherent quantum and diffusive classical nuclear motions (e and f, respectively). These non-Condon effects can be reflected in the spectrally integrated transients as modulations to the t-PL intensity that are either underdamped or overdamped (g and h, respectively).

molecular solvation dynamics (Figure 1f). A measurement of the time-domain signal in the case of a quantum mode creating strong non-Condon effects will arise as an amplitude modulation of either the dynamic absorption spectrum in TA or in the t-PL spectra, in contrast to the frequency modulation that is more commonly observed due to wavepacket motion (Figure 1g). In the case of the low-frequency classical mode undergoing solvation or glassy structural dynamics, there will be a time scale to the system response that is not instantaneous due to the importance of lattice geometry on the transition dipole moment in such a system (Figure 1h).

To obtain the highest signal-to-noise, we then focus on the spectrally integrated t-PL measurements on the time scale of 100 ps, with a 3 ps IRF. Figure 2a shows the t-PL data of 15

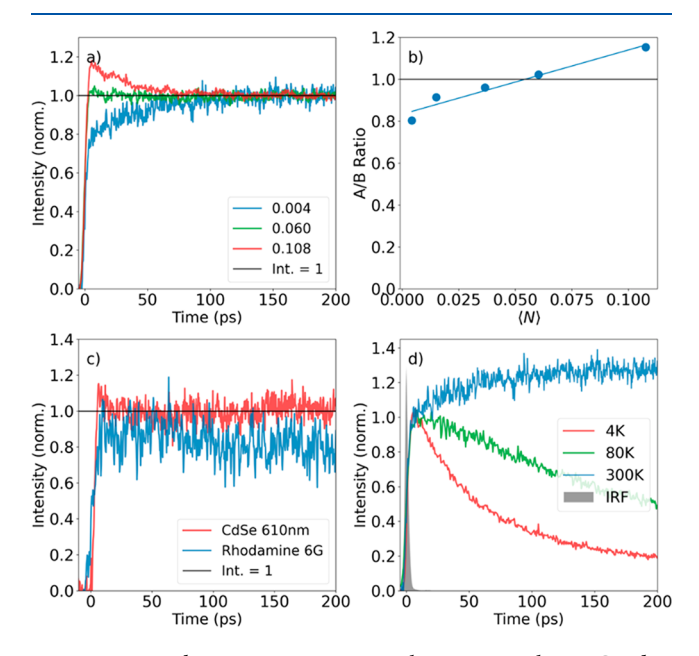


Figure 2. t-PL kinetic transients at early time reveal non-Condon effects in CsPbBr₃ perovskite nanocrystals. (a) The transients at very low exciton density, $\langle N \rangle \ll 1$. (b) The reciprocal saturation curve, showing the low exciton densities required to see the t-PL rise. The A/B ratio refers to the signal at time zero relative to the signal at 200 ps. (c) The t-PL transients in two reference systems with that are strongly covalent, thereby having quantum modes, including CdSe quantum dots and the molecular laser dye, rhodamine 6G. (d) There is a strong temperature dependence to the t-PL buildup in these MHP NC.

nm CsPbBr₃ MHP NC at various fluences that are low relative to the single exciton level normally used in nanocrystal and quantum dot spectroscopy, $\langle N \rangle < 1.$ In practice, that means that one typically uses fluences in which $\langle N \rangle \sim 0.3-0.5$ to observe linearity in the signals, especially in the TA signals. Here, we show that one can go to a low enough fluence to recover exponential kinetics of decay. But going to still lower fluences reveals a rise time to the buildup of the t-PL on the 30 ps time scale with a 20% amplitude. See the Supporting Information for details on the measurements of pulse energies, exciton densities, and fluence dependence. The fact that one must go to such extremely low exciton densities, $\langle N \rangle \sim 0.03$, reveals the strong probability of biexciton formation which creates fast signals that hide this t-PL buildup which is only observable at the absolute lowest of exciton densities.

To test if these effects were observable in other systems that are not glassy and ionic, we compared the t-PL to strongly covalent model chromophores of CdSe QD of 5.1 nm diameter and to rhodamine B laser dye in methanol (Figure 2c). Both of these are well-known chromophores and light emitters. Neither system shows any t-PL buildup, showing no evidence of non-Condon effects on this time scale. Nor is there any hot PL on this time scale for any system.

To test whether these effects are thermally assisted, the t-PL transients were obtained at 300, 80, and 4 K (Figure 2d). It is well-known that at low temperatures, perovskites show faster PL decays due to a faster radiative rate constant at low

temperature.²³ This increase in the rate constant at low temperatures is not well understood, however. Regardless, the fast decay at low temperature produces competition kinetics, which mask any possible buildup of PL due to non-Condon effects. At 80 K the data reveal a delayed decay rather than a buildup, and at 4 K there is a prompt decay due to the fast radiative decay.

In order to elucidate the origin of the non-Condon behavior of the PL in the CsPbBr₃ pervoskite, we perform *ab initio* modeling which provides a rationalization of the experimentally observed phenomenon. It has been established that metal halide perovskites (MHPs) are soft materials that can undergo significant structural changes when subjected to external perturbations, such as light, current, or temperature. MHP regions containing defects, such as point defects and grain boundaries, are particularly prone to such a response. 36–40

Building on our recent work on MHPs perovskite grain boundaries that can undergo both fast and slow structural changes, ^{38,39} we consider the response of such a system to photoexcitation (Figure 3). MHP samples contain surfaces,

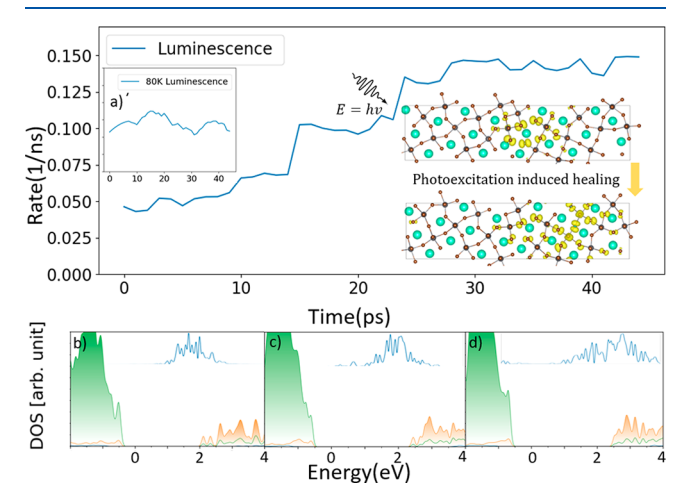


Figure 3. Results of *ab initio* and machine learning molecular dynamics simulations. (a) Evolution of luminescence in the $CsPbBr_3$ perovskite NC following photoexcitation at 300 K. The inset on the left shows the corresponding result at 80 K. The inset on the right demonstrated delocalization of the electron charge density at 300 K due to photoinduced defect heeling. Projected densities of states of the $CsPbBr_3$ perovskite NC at (b) 0, (c) 20, and (d) 40 ps after photoexcitation at 300 K. Green and orange denote contributions from Br and Pb atoms, respectively. Cs has little contribution in the shown energy range. The shallow trap states are healed, and the charge densities become more delocalized and shown in the insets, leading to an increase in the PL intensity.

boundaries, and edges that govern excited-state dynamics. 41-43 Such structures tend to create shallow states inside the fundamental bandgap, assisting exciton dissociation. The nanocrystals studied in this work contain a grain boundary and surfaces, while at the same time, the nanocrystal size is relatively small, and charges localized near such shallow defects interact due to quantum confinement effects.

We build the model of a typical grain boundary, equilibrate it at 80 and 300 K, as in the experiments, and consider the response to the photoexcitation (Figure 3). The simulation details and further data are shown in the Supporting Information. We do not consider 4 K because it is impossible

to define the simulation temperature to such fine accuracy due to finite size effects. In equilibrium at both 80 and 300 K, the system exhibits shallow trap states below the conduction band minimum (CBM) that localize electrons (Figure 3b). Similar, even more shallow, localized states appear at the valence band maximum (VBM) (Figure S1) such that the electron and hole overlap little, and the corresponding transition dipole moment is small (Figure S2).

Photoexcitation at 300 K facilitates healing of the shallow trap states, leading to charge delocalization, enhanced electron-hole overlap, increased transition dipole moment, and stronger PL. This effect is not observed at 80 K because at this temperature the system is more frozen and trapped in a local minimum structure. The structure changes little upon photoexcitation (Figure S4), the transition dipole moment remains the same (Figure S5), and the PL does not grow (Figure 3a inset). The simulations indicate that the PL decay observed experimentally at 4 and 80 K occurs as a result of excited-state depopulation. The rise in the PL signal observed at 300 K is due to structural dynamics in the excited state, on a time scale consistent with both the ultrafast diffraction experiments^{25,29} and the dielectric dispersion experiments in the THz regime.^{34,35,44} Such evolution facilitates healing of shallow traps present in MHPs, delocalizes electrons and holes, improves their overlap, and increases the PL transition dipole moment. At a long time, the PL decays both because of excited-state depopulation and relaxation of the MHP NC structure back to the local minima with shallow, localized charge trap states.

In summary, we find that metal halide perovskite nanocrystals display an anomalous photoluminescence time response, which shows an initial buildup rather than a prompt decay, as expected. This initial buildup of PL takes place on the time scale of 30 ps and is only visible near room temperatures at extremely low excitation levels and hence has never before been observed. This buildup of PL is assigned to a breakdown of the Condon approximation of a constant transition dipole moment, which is central to much spectroscopy, especially in the solid state. Theory at the *ab initio* molecular dynamics level is able to quantitatively reproduce the experimental observation in terms of excitation-induced structural dynamics.

ASSOCIATED CONTENT

Supporting Information

The Supporting Information is available free of charge at https://pubs.acs.org/doi/10.1021/acs.jpclett.3c02826.

Synthetic and experimental details, experimental details for t-PL spectroscopy and modeling (PDF)

Transparent Peer Review report available (PDF)

AUTHOR INFORMATION

Corresponding Author

Patanjali Kambhampati — Department of Chemistry, McGill University, Montreal, QC H3A 0G4, Canada; orcid.org/0000-0003-0146-3544; Phone: +1-514-398-7228; Email: pat.kambhampati@mcgill.ca

Authors

Dallas Strandell – Department of Chemistry, McGill University, Montreal, QC H3A 0G4, Canada

- Yifan Wu Department of Chemistry, University of Southern California, Los Angeles, California 90007, United States; orcid.org/0009-0006-3810-0885
- Carlos Mora-Perez Department of Chemistry, University of Southern California, Los Angeles, California 90007, United States
- Oleg Prezhdo Department of Chemistry, University of Southern California, Los Angeles, California 90007, United States; Occid.org/0000-0002-5140-7500

Complete contact information is available at: https://pubs.acs.org/10.1021/acs.jpclett.3c02826

Author Contributions

Experiments and analysis were done by D.S.; materials were synthesized and characterized by D.S.; calculations were done by Y.W., C.M.-P., and O.P.; the manuscript was written by D.S., O.P., and P.K.; P.K. supervised the work.

Funding

P.K. acknowledges financial support from NSERC, CFI, FQRNT, Sony Corporation, and McGill University. O.P. acknowledges support of the US National Science Foundation, Grant CHE-2154367.

Notes

The authors declare no competing financial interest.

REFERENCES

- (1) Mukamel, S. Principles of Nonlinear Optical Spectroscopy; Oxford University Press: 1995.
- (2) Tanimura, Y.; Mukamel, S. Temperature dependence and non-Condon effects in pump—probe spectroscopy in the condensed phase. *JOSA B* **1993**, *10* (12), 2263–2268.
- (3) Duque, J. G.; Chen, H.; Swan, A. K.; Shreve, A. P.; Kilina, S.; Tretiak, S.; Tu, X.; Zheng, M.; Doorn, S. K. Violation of the condon approximation in semiconducting carbon nanotubes. *ACS Nano* **2011**, *5* (6), 5233–5241.
- (4) Heller, E. J.; Yang, Y.; Kocia, L.; Chen, W.; Fang, S.; Borunda, M.; Kaxiras, E. Theory of graphene Raman scattering. *ACS Nano* **2016**, *10* (2), 2803–2818.
- (5) Henneker, W. H.; Siebrand, W.; Zgierski, M. Theory of resonance Raman scattering beyond the Condon approximation for a system with two modes of different symmetry. *J. Chem. Phys.* **1981**, 74 (12), 6560–6579.
- (6) Kumble, R.; Rush, T. S.; Blackwood, M. E.; Kozlowski, P. M.; Spiro, T. G. Simulation of non-condon enhancement and interference effects in the resonance Raman intensities of metalloporphyrins. *J. Phys. Chem. B* **1998**, *102* (37), 7280–7286.
- (7) Albrecht, A.; Clark, R. J.; Oprescu, D.; Owens, S. J.; Svendsen, C. Overtone resonance Raman scattering beyond the Condon approximation: Transform theory and vibronic properties. *J. Chem. Phys.* **1994**, *101* (3), 1890–1903.
- (8) Humeniuk, A.; Wohlgemuth, M.; Suzuki, T.; Mitrić, R. Timeresolved photoelectron imaging spectra from non-adiabatic molecular dynamics simulations. *J. Chem. Phys.* **2013**, *139* (13), No. 134104.
- (9) Kamarchik, E.; Krylov, A. I. Non-Condon effects in the one-and two-photon absorption spectra of the green fluorescent protein. *J. Phys. Chem. Lett.* **2011**, 2 (5), 488–492.
- (10) Tavernelli, I. Nonadiabatic molecular dynamics simulations: Synergies between theory and experiments. *Acc. Chem. Res.* **2015**, *48* (3), 792–800.
- (11) Tully, J. C. Nonadiabatic molecular dynamics. *Int. J. Quantum Chem.* **1991**, 40 (S25), 299–309.
- (12) Son, D. H.; Kambhampati, P.; Kee, T. W.; Barbara, P. F. Femtosecond multicolor pump— probe study of ultrafast electron transfer of [(NH3) SRuIIINCRuII (CN) 5]-in aqueous solution. *J. Phys. Chem. A* **2002**, *106* (18), 4591–4597.

- (13) Chen, T.-Y.; Hsia, C.-H.; Son, H. S.; Son, D. H. Ultrafast energy transfer and strong dynamic non-condon effect on ligand field transitions by coherent phonon in γ -Fe₂O₃ nanocrystals. *J. Am. Chem. Soc.* **2007**, *129* (35), 10829–10836.
- (14) Ishii, K.; Takeuchi, S.; Tahara, T. Pronounced Non-Condon Effect as the Origin of the Quantum Beat Observed in the Time-Resolved Absorption Signal from Excited-State cis-Stilbene. *J. Phys. Chem. A* **2008**, *112* (11), 2219–2227.
- (15) Sagar, D. M.; Cooney, R. R.; Sewall, S. L.; Dias, E. A.; Barsan, M. M.; Butler, I. S.; Kambhampati, P. Size dependent, state-resolved studies of exciton-phonon couplings in strongly confined semi-conductor quantum dots. *Phys. Rev. B: Condens. Matter Mater. Phys.* **2008**, 77 (23), No. 14235321.
- (16) Mooney, J.; Saari, J. I.; Kelley, A. M.; Krause, M. M.; Walsh, B. R.; Kambhampati, P. Control of Phonons in Semiconductor Nanocrystals via Femtosecond Pulse Chirp-Influenced Wavepacket Dynamics and Polarization. *J. Phys. Chem. B* **2013**, *117* (49), 15651.
- (17) Palato, S.; Seiler, H.; Nijjar, P.; Prezhdo, O.; Kambhampati, P. Atomic fluctuations in electronic materials revealed by dephasing. *Proc. Natl. Acad. Sci. U. S. A.* **2020**, 117 (22), 11940.
- (18) Green, M. A.; Ho-Baillie, A.; Snaith, H. J. The Emergence of Perovskite Solar Cells. *Nat. Photonics* **2014**, *8*, 506.
- (19) Stranks, S. D.; Snaith, H. J. Metal-halide perovskites for photovoltaic and light-emitting devices. *Nat. Nanotechnol.* **2015**, *10* (5), 391.
- (20) Akkerman, Q. A.; Rainò, G.; Kovalenko, M. V.; Manna, L. Genesis, Challenges and Opportunities for Colloidal Lead Halide Perovskite Nanocrystals. *Nat. Mater.* **2018**, *17*, 394.
- (21) Kovalenko, M. V.; Protesescu, L.; Bodnarchuk, M. I. Properties and Potential Optoelectronic Applications of Lead Halide Perovskite Nanocrystals. *Science* **2017**, *358*, 745.
- (22) Protesescu, L.; Yakunin, S.; Bodnarchuk, M. I.; Krieg, F.; Caputo, R.; Hendon, C. H.; Yang, R. X.; Walsh, A.; Kovalenko, M. V. Nanocrystals of Cesium Lead Halide Perovskites (CsPbX3, X = Cl, Br, and I): Novel Optoelectronic Materials Showing Bright Emission with Wide Color Gamut. *Nano Lett.* **2015**, *15*, 3692.
- (23) Dey, A.; Ye, J.; De, A.; Debroye, E.; Ha, S. K.; Bladt, E.; Kshirsagar, A. S.; Wang, Z.; Yin, J.; Wang, Y.; Quan, L. N.; Yan, F.; Gao, M.; Li, X.; Shamsi, J.; Debnath, T.; Cao, M.; Scheel, M. A.; Kumar, S.; Steele, J. A.; Gerhard, M.; Chouhan, L.; Xu, K.; Wu, X.-g.; Li, Y.; Zhang, Y.; Dutta, A.; Han, C.; Vincon, I.; Rogach, A. L.; Nag, A.; Samanta, A.; Korgel, B. A.; Shih, C.-J.; Gamelin, D. R.; Son, D. H.; Zeng, H.; Zhong, H.; Sun, H.; Demir, H. V.; Scheblykin, I. G.; Mora-Seró, I.; Stolarczyk, J. K.; Zhang, J. Z.; Feldmann, J.; Hofkens, J.; Luther, J. M.; Pérez-Prieto, J.; Li, L.; Manna, L.; Bodnarchuk, M. I.; Kovalenko, M. V.; Roeffaers, M. B. J.; Pradhan, N.; Mohammed, O. F.; Bakr, O. M.; Yang, P.; Müller-Buschbaum, P.; Kamat, P. V.; Bao, Q.; Zhang, Q.; Krahne, R.; Galian, R. E.; Stranks, S. D.; Bals, S.; Biju, V.; Tisdale, W. A.; Yan, Y.; Hoye, R. L. Z.; Polavarapu, L. State of the Art and Prospects for Halide Perovskite Nanocrystals. ACS Nano 2021, 15 (7), 10775–10981.
- (24) Wang, F. F.; Fu, Y. P.; Ziffer, M. E.; Dai, Y. N.; Maehrlein, S. F.; Zhu, X. Y. Solvated Electrons in Solids-Ferroelectric Large Polarons in Lead Halide Perovskites. *J. Am. Chem. Soc.* **2021**, *143* (1), 5.
- (25) Guzelturk, B.; Winkler, T.; Van de Goor, T. W. J.; Smith, M. D.; Bourelle, S. A.; Feldmann, S.; Trigo, M.; Teitelbaum, S. W.; Steinrück, H.-G.; de la Pena, G. A.; Alonso-Mori, R.; Zhu, D.; Sato, T.; Karunadasa, H. I.; Toney, M. F.; Deschler, F.; Lindenberg, A. M. Visualization of dynamic polaronic strain fields in hybrid lead halide perovskites. *Nat. Mater.* **2021**, *20* (5), 618–623.
- (26) Miyata, K.; Meggiolaro, D.; Trinh, M. T.; Joshi, P. P.; Mosconi, E.; Jones, S. C.; De Angelis, F.; Zhu, X.-Y. Large Polarons in Lead Halide Perovskites. *Sci. Adv.* **2017**, *3*, No. e1701217.
- (27) Miyata, K.; Atallah, T. L.; Zhu, X. Y. Lead Halide Perovskites: Crystal-Liquid Duality, Phonon Glass Electron Crystals, and Large Polaron Formation. *Sci. Adv.* **2017**, *3*, No. e1701469.
- (28) Seiler, H.; Palato, S.; Sonnichsen, C.; Baker, H.; Socie, E.; Strandell, D. P.; Kambhampati, P. Two-dimensional electronic

- spectroscopy reveals liquid-like lineshape dynamics in CsPbI3 perovskite nanocrystals. *Nat. Commun.* **2019**, *10*, 4962.
- (29) Wu, X. X.; Tan, L. Z.; Shen, X. Z.; Hu, T.; Miyata, K.; Trinh, M. T.; Li, R. K.; Coffee, R.; Liu, S.; Egger, D. A.; Makasyuk, I.; Zheng, Q.; Fry, A.; Robinson, J. S.; Smith, M. D.; Guzelturk, B.; Karunadasa, H. I.; Wang, X. J.; Zhu, X. Y.; Kronik, L.; Rappe, A. M.; Lindenberg, A. M. Light-induced picosecond rotational disordering of the inorganic sublattice in hybrid perovskites. *Sci. Adv.* **2017**, 3 (7), No. e1602388.
- (30) Schilcher, M. J.; Robinson, P. J.; Abramovitch, D. J.; Tan, L. Z.; Rappe, A. M.; Reichman, D. R.; Egger, D. A. The Significance of Polarons and Dynamic Disorder in Halide Perovskites. *Acs Energy Letters* **2021**, *6* (6), 2162.
- (31) Yaffe, O.; Guo, Y. S.; Tan, L. Z.; Egger, D. A.; Hull, T.; Stoumpos, C. C.; Zheng, F.; Heinz, T. F.; Kronik, L.; Kanatzidis, M. G.; Owen, J. S.; Rappe, A. M.; Pimenta, M. A.; Brus, L. E. Local Polar Fluctuations in Lead Halide Perovskite Crystals. *Phys. Rev. Lett.* **2017**, *118* (13), No. 136001.
- (32) Li, W.; She, Y.; Vasenko, A. S.; Prezhdo, O. V. Ab initio nonadiabatic molecular dynamics of charge carriers in metal halide perovskites. *Nanoscale* **2021**, *13* (23), 10239–10265.
- (33) Chu, W.; Zheng, Q.; Prezhdo, O. V.; Zhao, J.; Saidi, W. A. Low-frequency lattice phonons in halide perovskites explain high defect tolerance toward electron-hole recombination. *Sci. Adv.* **2020**, *6* (7), No. eaaw7453.
- (34) Ghosh, A.; Strandell, D. P.; Kambhampati, P. A spectroscopic overview of the differences between the absorbing states and the emitting states in semiconductor perovskite nanocrystals. *Nanoscale* **2023**, *15*, 2470.
- (35) Kambhampati, P. Learning about the Structural Dynamics of Semiconductor Perovskites from Electron Solvation Dynamics. *J. Phys. Chem. C* **2021**, *125* (43), 23571–23586.
- (36) Cohen, A. V.; Egger, D. A.; Rappe, A. M.; Kronik, L. Breakdown of the static picture of defect energetics in halide perovskites: the case of the Br vacancy in CsPbBr3. *J. Phys. Chem. Lett.* **2019**, *10* (16), 4490–4498.
- (37) Chu, W.; Saidi, W. A.; Zhao, J.; Prezhdo, O. V. Soft lattice and defect covalency rationalize tolerance of β -CsPbI3 perovskite solar cells to native defects. *Angew. Chem., Int. Ed.* **2020**, 59 (16), 6435–6441.
- (38) Wu, Y.; Liu, D.; Chu, W.; Wang, B.; Vasenko, A. S.; Prezhdo, O. V. Fluctuations at Metal Halide Perovskite Grain Boundaries Create Transient Trap States: Machine Learning Assisted Ab Initio Analysis. ACS Appl. Mater. Interfaces 2022, 14 (50), 55753–55761.
- (39) Liu, D.; Wu, Y.; Vasenko, A. S.; Prezhdo, O. V. Grain boundary sliding and distortion on a nanosecond timescale induce trap states in CsPbBr 3: ab initio investigation with machine learning force field. *Nanoscale* **2022**, *15* (1), 285–293.
- (40) Wang, B.; Chu, W.; Wu, Y.; Casanova, D.; Saidi, W. A.; Prezhdo, O. V. Electron-volt fluctuation of defect levels in metal halide perovskites on a 100 ps time scale. *J. Phys. Chem. Lett.* **2022**, *13* (25), 5946–5952.
- (41) Zhang, Z.; Fang, W.-H.; Long, R.; Prezhdo, O. V. Exciton dissociation and suppressed charge recombination at 2D perovskite edges: key roles of unsaturated halide bonds and thermal disorder. *J. Am. Chem. Soc.* **2019**, *141* (39), 15557–15566.
- (42) Shi, R.; Vasenko, A. S.; Long, R.; Prezhdo, O. V. Edge influence on charge carrier localization and lifetime in CH3NH3PbBr3 perovskite: Ab initio quantum dynamics simulation. *J. Phys. Chem. Lett.* **2020**, *11* (21), 9100–9109.
- (43) Lu, J.; Zhou, C.; Chen, W.; Wang, X.; Jia, B.; Wen, X. Origin and physical effects of edge states in two-dimensional Ruddlesden-Popper perovskites. *iScience* **2022**, 25, 104420.
- (44) Herz, L. M. How Lattice Dynamics Moderate the Electronic Properties of Metal-Halide Perovskites. *J. Phys. Chem. Lett.* **2018**, 9 (23), 6853.